Highly weathered mineral soils have highest transfer risk of radiocaesium contamination after a nuclear accident: A global soil-plant study

Margot Vanheukelom [a,b,*], Lieve Sweeck [a], Talal Almahayni [a], Mara De Bruyn [a,b], Pieter Steegmans [a,b], Lore Fondu [b], Axel Van Gompel [a], May Van Hees [a], Jean Wannijn [a], Erik Smolders [b]
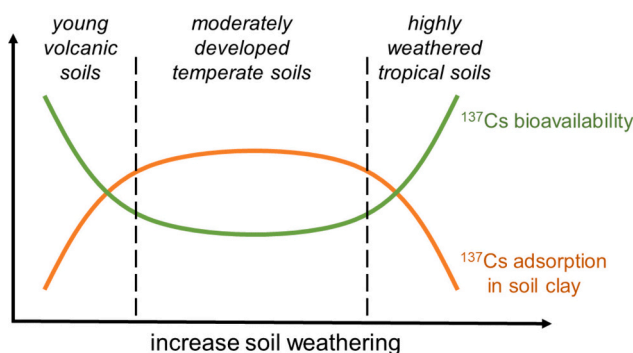
[a] Biosphere Impact Studies, Belgian Nuclear Research Centre (SCK CEN), Boeretang 200, 2400 Mol, Belgium
[b] Division of Soil and Water Management, KU Leuven, Kasteelpark Arenberg 20, 3001 Leuven, Belgium

HIGHLIGHTS

- ^{137}Cs soil-to-plant transfer models are not calibrated for soils on global scale.
- Young and highly weathered soils without 2:1 clay adsorb least ^{137}Cs per unit clay.
- Pot trial ^{137}Cs transfer factors for grass vary 10,000–fold among soils.
- ^{137}Cs soil-to-plant transfer was highest in highly weathered soils.
- Tarsitano (2011) model predicts ^{137}Cs soil-to-plant transfer ($R^2 = 0.8$, 3–fold deviation).

GRAPHICAL ABSTRACT

ABSTRACT

Accidental release of radiocaesium (^{137}Cs) from nuclear power plants may result in long-term contamination of environmental and food production systems. Assessment of food chain contamination with ^{137}Cs relies on ^{137}Cs soil-to-plant transfer data and models mainly available for regions affected by the Chornobyl and Fukushima accidents. Similar data and models are lacking for other regions. Such information is needed given the global expansion of nuclear energy. We collected 38 soils worldwide of contrasting parent materials and weathering stages. The soils were spiked with ^{137}Cs and sown with ryegrass in greenhouse conditions. The ^{137}Cs grass-soil concentration ratio varied four orders of magnitude among soils. It was highest in Ferralsols due to the low ^{137}Cs interception potential of kaolinite clay and the low exchangeable potassium in these soils. Our results demonstrate, for the first time, the high plant uptake of ^{137}Cs in tropical soils. The most recent ^{137}Cs transfer model, mainly calibrated to temperate soils dominated by weathered micas, poorly predicts the underlying processes in tropical soils but, due to compensatory effect, still reasonably well predicts ^{137}Cs bioavailability across all soils ($R^2 = 0.8$ on a log-log scale).

1. Introduction

Caesium–137 (^{137}Cs) is one of the most critical radionuclides released after nuclear accidents because of its long half-live (30 years) and its similarity to potassium (K), which makes it easy to enter the human food chain. Decision-makers rely on ^{137}Cs soil-to-plant transfer data and models to predict the concentrations of ^{137}Cs entering the food chain. Although models were developed after the Chornobyl and Fukushima accidents to predict ^{137}Cs transfer to plants for European and Japanese soils, there is a need for transfer models applicable to other (e. g. tropical) regions, as the use of nuclear power increases worldwide.

The transfer of ^{137}Cs, expressed as the concentration ratio (CR) of ^{137}Cs in plants to that in soil, shows substantial variation. The IAEA compiled ^{137}Cs CR values for grass, ranging from 10^{-4} to 10 kg kg^{-1} (IAEA, 2021; IAEA, 2020; IAEA, 2009), with no clear explanation based on soil texture (e.g. sand, loam, clay) (Almahayni et al., 2019). After the Chornobyl accident, the highest soil-to-plant transfer of ^{137}Cs was observed in peatlands because peat soils are devoid of clay minerals, which selectively retain ^{137}Cs. Greenhouse studies confirmed exceptionally large CR values, often >1 kg kg^{-1}, for plants grown in peat (Sanchez et al., 1999). Further research revealed that ^{137}Cs uptake in plants is controlled by the ratio of ^{137}Cs and K in soil solution (Smolders et al., 1997). Both elements use the same uptake systems in plant roots (Zhu and Smolders, 2000). Predicting soil ^{137}Cs transfer to plants requires considering Cs:K competition at the soil-root interface and ^{137}Cs adsorption to soil particles. The retention of ^{137}Cs in soil takes place on the Cs selective binding sites called Frayed Edge Sites (FES), quantified using Radiocaesium Interception Potential (RIP), which combines the selectivity coefficient of Cs relative to K and the FES capacity of the soil (Cremers et al., 1988).

The lack of ^{137}Cs soil-to-plant transfer models calibrated for regions outside Europe and Japan remains a concern. Existing models (Absalom et al., 1999, 2001; Tarsitano et al., 2011) do not account for the effect of soil mineralogy on the ^{137}Cs transfer to plants. Furthermore, model parameters are lacking for highly weathered soils prevalent in tropical regions. A recent pot trial showed nearly two orders of magnitude variation in ^{137}Cs CR among synthetic soils prepared by mixing sand with different clay minerals (Vanheukelom et al., 2022) and showed that next to exchangeable K and clay content, the type of minerals matters for ^{137}Cs bioavailability. Global diversity in soil mineralogy challenges assumptions of these models, particularly regarding the 2:1 phyllosilicates with high FES fractions found at intermediate weathering stages, whereas they are smaller in very young (e.g. volcanic) soils and almost absent in highly weathered stages dominated by 1:1 phyllosilicates.

This study aimed to measure the CR values of ^{137}Cs in soils with diverse mineralogies at varying stages of development and to validate the extent to which existing models can realistically predict ^{137}Cs transfer from these soils. Two soil sequences were sampled representing different weathering stages affecting soil mineralogy. In addition, 26 other soils with contrasting soil properties, covering Andosol to Ferralsol, were included in the collection. A greenhouse experiment was set up with these soils. A subset of the soils was fertilized without and with K to investigate its effect on ^{137}Cs CR reduction. The soils were characterized, spiked with ^{137}Cs and grown with grass.

2. Materials and methods

2.1. Soil collection

Topsoils (0–20 cm) came from 6 locations of a sequence in Kenya, 6 locations of a sequence in Philippines and 26 locations worldwide (Fig. A1; Table A.1). The soils were classified according to the World Reference Base for Soil Resource (IUSS Working Group WRB, 2022) or derived from the 250 m gridded world map SoilGrids™ (https://soilgrids.org) based on the geo-referenced location. The soils covered nine Köppen-Geiger climate subgroups (Beck et al., 2018) and fourteen major WRB soil classes.

2.2. Soil characterization

Subsamples of air-dried soil, sieved at 2 mm, were used for characterization. All air-dry soil weights were corrected for moisture content (105 °C). Particle size distribution was determined by laser diffraction. Subsamples of 5 g were taken using a sample splitter and put in deionized water. Carbonates were removed using 3 mol L^{-1} HCl, and organic matter was removed using 3 mol L^{-1} H$_2$O$_2$ in doses until the reaction ceased. Before measurement, the particles were ultrasonically dispersed. For Ferralsol samples, iron (hydr)oxides were removed using 10 mL of 0.56 mol L^{-1} oxalic acid. One Ferralsol was re-measured to compare the effect of iron removal and ultrasonic dispersion (Table A.5). Particles were measured by laser diffraction (LS 13320, Beckman Coulter). For a selection of samples ($N = 28$), the particle size distribution was also determined by the pipette method (ISO 11277, 1998) without iron removal. All fractional weights were corrected for losses and normalized to percentages. As the particle size distributions yielded different results depending on the method, the highest clay content was used for modelling unless stated otherwise. The total carbon and organic carbon (C) contents were determined by dry combustion. Organic C samples were acidified with 3 mol L^{-1} HCl and dried (50 °C). Carbon release was measured upon combustion (900 °C) (EA 1108, Carlo Erba). Inorganic C was calculated as the difference in %C between total C and organic C.

Soil mineralogy was determined on bulk powder samples with added standard by X-ray diffraction (XRD) (Środoń et al., 2001; Zeelmaekers, 2011). Oven-dried (60 °C) soils were crushed by pestle and mortar until all material passed through a 0.5 mm sieve. Soil (90 wt%) and zincite standard (10 wt%) were analytically weighted and wet-milled (McCrone Micronizing Mill) in ethanol for 7 min to obtain a homogenous mixture. Mixtures were placed under a fume hood until dry. The powder was passed through a 0.355 mm sieve. The powder was inserted in a side-loading holder. Measurements were carried out with two diffractometers in Bragg-Brentano arrangements with Cu-K$_\alpha$ radiation: with 173 mm goniometer radius, a graphite crystal monochromator, a gas proportional detector scanning at 45 kV and 30 mA, ranging over 5–65°2θ with 0.02°2θ step size and 2 s counting time (PW1830, Philips), or with 250 mm radius, a variable divergence slit, two solar slits, a position sensitive detector (LynxEye, Bruker) scanning at 40 kV and 40 mA over 3–75°2θ at 0.01°2θ in 0.2 s (D8 Advance, Bruker). The minerals in the powder were identified and quantified using two methods belonging to the respective diffractometers. Quanta software (© Chevron ETC) used the Mineral Intensity Factors method (Moore and Reynolds, 1997), where the sum of single reflections of the mineral phases was fitted to the recorded XRD pattern. Profex software (version 5.2.0) (Doebelin and Kleeberg, 2015) used the Rietveld method, where the whole pattern simulated by calibrated crystallographic parameters is fitted to the recorded pattern. Seven samples were measured and processed independently using two setups for comparison (Table A.2), but patterns of the former diffractometer and method were used for data analysis. The soil weathering index (*WI*) was calculated (Table A.2):

$$WI = \sum_{i=1}^{12} \%m \bullet i$$

where *%m* represents the percentage of each mineral phase in the bulk soil, and *i* represents the index (*i*) of weatherability of the corresponding mineral (Jackson et al., 1948; Jackson and Sherman, 1953). The weathering index of minerals ranges from 1 to 12, with 1 indicating the youngest mineral (e.g. gypsum) and 12 the most stable mineral (e.g. anatase).

The cation exchange capacity (CEC) was determined using cobalt hexamine (Ciesielski and Sterckeman, 1997). Samples of air-dry soil with 16.6 mmol L^{-1} Co(NH$_3$)$_6$Cl$_3$ were shaken end-over-end (1 h). After centrifugation (15 min), the supernatant was filtered at 0.45 μm

(Acrodisc®). The cation concentrations were measured (7700 Series ICP-MS, Agilent Technologies; 4200 MP-AES, Agilent Technologies). The CEC was calculated as the difference between the initial and final Co equivalent charge concentration in solution per soil weight.

The RIP of the soils was determined by exchanging ^{137}Cs with K–cations on the selective adsorption sites while blocking non-selective sites with Ca–cations (Wauters et al., 1996). Samples of 1 g air-dry soil in dialysis membrane bags (VISKING®, MWCO 12–14 kDa; Spectra/Por®, MWCO 6–8 kDa) with 10 mL of 0.5 mmol L^{-1} K and 100 mmol L^{-1} Ca solution were placed in pots containing 150 mL K–Ca solution, and shaken end-over-end (24 h). The outer K—Ca solution was renewed and shaken (24 h). Next, the outer solution was renewed with 200 kBq mL^{-1} ^{137}Cs with K—Ca solution and shaken (24 h). The ^{137}Cs concentration in the initial and final outer solution was measured with a gamma counter (1480 WIZARD 3″, Perkin Elmer). The RIP was calculated by multiplying the measured ^{137}Cs solid-liquid distribution with 0.5 mmol L^{-1} K in solution.

2.3. Pot experiment

The experiment included two sets of soil batches taken worldwide (experiment A, $N = 26$) and from sequences (experiment B, performed after experiment A, $N = 12$). Air-dry soils were sieved at 4 mm, and about 3 kg soil was transferred to buckets before fertilization and spiking (Fig. A.3). Carrier-free ^{137}CsCl was added at a rate of 400 kBq kg^{-1}. All soils were NP–fertilized. Three soils with low K–buffering capacity in experiment A (a sandy, a volcanic, and a tropical soil) and the sequences in experiment B were subjected to two K fertilizer treatments: without (no K, $N = 38$) and with (+K, $N = 15$) fertilizer. Fertilizer, including NH$_4$NO$_3$, NaH$_2$PO$_4$•H$_2$O and MgSO$_4$•7H$_2$O, was added at rates of 50 mg N–NO$_3$ kg^{-1}, 50 mg N–NH$_4$ kg^{-1}, 13 mg P kg^{-1}, 16 mg S kg^{-1}, and 12 mg Mg kg^{-1}. In the case of Ferralsols, where extremely high phosphorus sorption on iron-containing (oxyhydr)oxides is typical (De Bauw et al., 2021), 5 g of granules containing 46 % Ca(H$_2$PO$_4$)$_2$•H$_2$O were added per pot to reach a final P dose of 57 mg P kg^{-1} (with 6 mg K kg^{-1} as impurity). Additional KCl was added to the 15 soils with the +K treatment at a rate of 150 mg K kg^{-1}. The fertilizer as stock solution together with the ^{137}Cs in deionized water were added to the soil to obtain 50 % of the moisture content of a fully saturated soil, the latter was determined by the saturated paste method (USDA, 1954). The soils were incubated in covered buckets at room temperature for 14 days, during which deionized water was added to correct for weight loss, and soils were mixed with spatulas every 2–3 days. Soil moisture content was increased to 55 % (Cavinti to 75 %; Luisana to 85 %) using deionized water for at least 7 days for solution separation.

Soil solution was separated by centrifugation. The moist soils were placed in an in-house made two-compartment cup, which featured a 2.5 μm filter (Whatman®) placed on a porous plate, separating the soil from the solution. After centrifugation (30 min), the solution collected in the lower compartment was filtered at 0.45 μm. The separation process took about 20 days to ensure that a sufficient volume of solution was obtained from each of the soils (Fig. A.3). Soils were mixed and deionized water was added. The ^{137}Cs concentration in soil solution was determined with a NaI(Tl) scintillation gamma counter (measuring time 10–50 min, average counting efficiency ~16 %;1480 WIZARD 3″, Perkin Elmer). Samples with too low ^{137}Cs concentrations (i.e. below the detection limit of the NaI(Tl) counter) were measured using a high purity germanium gamma detector (16–24 h, efficiency ~10–40 %; SEGe, Canberra). The K, Na, Ca and Mg concentrations were measured using ICP-MS. The NH$_4$ concentration was measured colorimetrically (SA 40, Skalar).

Before potting the soil, subsamples were taken to analyze the soil pH, total ^{137}Cs content, and exchangeable cations. The soil pH was determined in diluted CaCl$_2$ suspension (Schofield et al., 1955). Samples of 5 g air-dry soil in 12.5 mL of 0.01 mol L^{-1} CaCl$_2$ were shaken end-over-end (2 h) and pH measured (PC 5000 L, pHenomenal®). The total soil ^{137}Cs concentration was determined by measuring air-dry soil samples with a gamma counter. Exchangeable cations in soil were determined using ammonium acetate. Samples of 1 g air-dry soil in 18 mL of 1 mol L^{-1} NH$_4$CH$_3$COO were shaken end-over-end (24 h). After centrifugation (15 min), the supernatant was filtered at 0.45 μm. The ^{137}Cs concentration in supernatant was determined with a gamma counter. The K, Na, Ca and Mg concentrations were measured using MP-AES. Only in experiment A ($N = 29$) the exchangeable NH$_4$ was determined following the same procedure, but instead 1 mol L^{-1} KCl was used. The NH$_4$ concentration in the supernatant was measured colorimetrically. In experiment B ($N = 24$), samples of the sequence soils were taken after plant growth to measure exchangeable ^{137}Cs, K, Na, Ca and Mg.

After the 42–45 days pre-incubation period, soils were divided over three 1 L pots, which were filled to an equal volume. Per pot, 0.65 g seeds of grass (*Lolium perenne* L.) were sown by spreading seeds on the surface, at least 1 cm from the rim and buried under about 60 g soil. The pots were covered until germination to prevent excessive drying of the soil. Cultivation was carried out in a growing chamber with a day/night rhythm of 14/10 h at 24/18 °C. The pots were watered (~50 % moisture content) with deionized water every 2–3 days based on weight loss and pot positions were randomized. Grass shoots were harvested after 30 days. The above-ground plant material was cut off 1 cm above the surface to prevent ^{137}Cs contamination from the soil. The fresh weight of the plant material was recorded. The dry weight was recorded after drying the plant material in the oven (65 °C) for 6 days. The shoots were calcinated (550 °C), ash was dissolved in 2 mL of 12 mol L^{-1} HCl, calcinated again and dissolved in diluted 0.1 mol L^{-1} HCl. The ^{137}Cs concentrations were analyzed with a NaI(Tl) or Ge detector. The K, Na, Ca and Mg concentrations were measured with ICP-MS or MP-AES. The concentration ratio (CR), was calculated as

$$CR = \frac{^{137}\text{Cs in grass shoots} \left(\frac{\text{Bq}}{\text{kg shoot}} \right)}{^{137}\text{Cs in soil} \left(\frac{\text{Bq}}{\text{kg soil}} \right)}$$

with both concentrations reported on a dry-weight basis. The concentration factor (CF) was calculated as

$$CF = \frac{^{137}\text{Cs in grass shoots} \left(\frac{\text{Bq}}{\text{kg shoot}} \right)}{^{137}\text{Cs in soil solution} \left(\frac{\text{Bq}}{\text{L soil solution}} \right)}$$

with dry-weight shoots.

2.4. Statistical analyses

JMP® Pro software (Version 17.0.0 SAS Institute Inc., Cary, NC, 1989–2023) was used. Standard deviations of the CR and CF values were derived using error propagation formula because soil, solution and plant samples were not paired. Variables with skewness >0.5 were log-transformed unless stated otherwise. Significant differences in dry-weight grass yields among experiments A and B were tested using a non-parametric Wilcoxon Rank-Sum at a 5 % significance level. Significant differences between replicate ^{137}Cs CR values among soils were tested using a Tukey-Kramer HSD test at a 5 % significance level for equal sample sizes. Significant differences in dry-weight grass yields and ^{137}Cs CR values among texture/organic C/pH groups or WRB soil class groups were tested using a non-parametric comparison for all pairs Dunn's test at a 5 % significance level. Pearson correlation coefficients were calculated on the log-transformed means ($n = 3$), except for pH, which is inherently on a log-scale (Table A.8; Table A.9). Multiple linear regression was used, taking into account interaction-effects ($p < 0.05$), to obtain relations describing CR with selected explanatory variables.

3. Results

3.1. Soil properties

The soils differed in their physico-chemical properties and the stage of weathering (Table 1; Table A.2). Soils had various properties with clay contents ranging between 2.8 % and 83 %, soil pH ranging over 3.0–7.8, soil organic C contents (%SOC) ranging over 0.23–14 % and CEC ranging over 1.9–91 $cmol_c$ kg^{-1}. The Kenyan soil sequence developed from volcanic ash showed a gradient in weathering index ranging over 3.7–7.9 from young, organic soils on the mountain to more weathered clayey soils in the valley with components such as kaolinite (6–24 %), but also 2:1 phyllosilicates (6–16 %) increasing in concentration. The Philippine sequence with weathering indexes ranging over 4.6–9.2 was dominated by kaolinite (15–68 %), which became more abundant as weathering increased. In parallel, soil originating from volcanic ashes in Miyakonojo (Japan) was at an early stage of development (Shoji and Takahashi, 2002) and contained mainly allophane and feldspar. It also included some muscovite (7 %), which was not derived from volcanic ash, but from mica-bearing aeolian deposits from Chinese deserts (Nakao et al., 2021). Soils from sedimentary parent material in Europe, such as loess deposits, were moderately developed which contained 2:1 phyllosilicates (up to 50 %) and some kaolinite (<20 %). Soils from volcanic plateaus in Behenjy (Madagascar) and Luisiana (Philippines) were highly weathered and contained mainly kaolinite (>30 %).

The yields of clay content were compared among different particle size distribution methods. For one Ferralsol, iron removal and ultrasonic dispersion treatments before laser diffraction measurement were compared (Table A.5). The clay content ranged from 30 % to 44 %, depending on the dispersion treatment, indicating the slight sensitivity of the procedural difference in this method. However, a much higher clay content of 83 % was found following the standard pipette method without iron removal (ISO 11277) on the same soil (Table A.5). Clay yield differences after the pipette and laser diffraction methods were also found for other soils. In the following sections, the highest clay content determined for each soil was used, usually the pipette method, because it best matched the total phyllosilicate content after XRD (Fig. A.7(b)).

The muscovite and 2:1 phyllosilicate content explained 52 % of the variability in soil RIP ($R^2 = 0.52$, root mean square error (RMSE) = 0.43, $N = 38$). Soil RIP was low in the youngest, volcanic soil (Andosols), but increased up to 50–fold in the more developed soils (Kastanozem/

Chernozem/Phaeozem), and decreased again up to 440–fold in the weathered, tropical soil (Ferralsols) (Table A.3). Furthermore, the geometric mean (GM) of the RIP per unit clay was generally low in the Andosols and Ferralsols (<1000 mmol kg^{-1} clay) compared to the moderately weathered soils (25,600 mmol kg^{-1} clay) (Table 1; Fig. A.4). These findings suggest that the mineralogy and the weathering stage of the soil partially controlled the RIP in our study. A similar trend emerged for the CEC: this was low for the Andosol despite the high clay content and organic matter (Table 1), the CECs of the more developed soils were higher, except the sandy soils, and the CEC of the Ferralsols was low despite the high clay contents.

3.2. Pot experiment

The shoot yield averaged 0.73 g dry weight per pot among all soils and treatments (Table A.7). Yield ranged from 0.044 g to 2.9 g and was significantly higher ($p < 0.05$) in experiment B (1.5 ± 0.6 g, mean ± standard deviation) compared to experiment A (0.56 ± 0.36 g), likely because seeds used for A were 3 years older than those for B. Dry matter yields were unaffected ($p > 0.05$) by WRB soil class groups or single soil properties. No significant correlations were found between yield and ^{137}Cs CR (Table A.8). The ^{137}Cs CR ranged over 4 orders of magnitude between 0.0047 and 47 kg kg^{-1} (Fig. 1; Fig. A.4; Table A.7). The exchangeable K content in soils before plant growth within a soil class group varied up to 29–fold (Ferralsols, no K) (Fig. A.4; Table A.6). The ^{137}Cs CR was significantly ($p < 0.05$) affected by the soil and treatment, as the log CR values of the replicates differed for 20 out of 53 treated soils (Table A.7). However, neither the soil classification based on clay, sand and organic matter contents (IAEA, 2009) nor the WRB soil class grouping explained the log CR values ($p > 0.05$).

3.3. K addition lowered ^{137}Cs transfer

Adding K (150 mg kg^{-1} equivalent to 0.38 $cmol_c$ kg^{-1}) reduced the CR values up to 24–fold (Gleysol) (Fig. A.6). Despite the reduction of ^{137}Cs transfer to grass by adding K, CR is still high (>0.1 kg kg^{-1}) for the young, volcanic soil (Andosol), the sandy soil (Anthrosol), and the weathered tropical soil (Ferralsol) with low initial exchangeable K content (<0.5 $cmol_c$ kg^{-1}) and low K solid-liquid distribution coefficient ($K_D < 5$ L kg^{-1}). Adding K was not effective in soils (Nitisols) with a high initial exchangeable K content (>2.0 $cmol_c$ kg^{-1}).

Table 1

Summary of selected characteristics of the soils. More details are in the Supplementary information (Table A.3).

Soil classes[a]	N[b]	clay[c]			SOC[d]			CEC[e]			RIP per unit clay[f]			Weathering index		
WRB		%			%			$cmol_c$ kg^{-1} soil			mmol kg^{-1} clay			–		
		min	max	GM	min	max	GM	min	max	GM	min	max	GM	min	max	GM
Andosol	2	23	34	28	5.6	14	8.7	5.1	6.2	5.6	502	1080	738	2.5	3.7	3.0
Kastanozem/Chernozem/Phaeozem	3	18	24	21	1.0	1.4	1.2	13	33	21	17,500	29,400	21,900	4.8	5.8	5.2
Fluvisol	3	10	14	12	0.87	1.0	0.94	17	91	50	21,600	32,300	25,600	5.4	5.6	5.5
Gleysol	2	22	32	26	1.3	1.8	1.5	5.4	32	13	2340	6300	3840	5.2	6.1	5.6
Luvisol/Lixisol	3	6.0	27	13	0.45	1.3	0.88	2.9	20	9.4	12,900	27,900	19,200	5.5	6.0	5.7
Nitisol	2	42	46	44	5.3	8.4	6.7	46	50	48	3980	10,900	6580	5.1	6.6	5.8
Anthrosol	2	2.8	6.0	4.1	2.3	2.9	2.6	1.9	9.2	4.2	3000	18,000	7340	5.9	6.0	5.9
Cambisol	10	5.7	49	27	0.23	2.3	1.3	8.4	34	21	1700	20,200	6000	4.6	7.6	6.1
Vertisol	3	32	39	35	1.2	2.0	1.6	19	26	22	3680	14,900	6380	6.0	7.1	6.6
Acrisol	5	14	62	29	0.56	3.7	1.9	9.9	84	34	209	15,300	3970	6.1	9.2	6.9
Ferralsol	3	42	83	61	0.54	2.9	1.4	2.3	8.3	5.2	32.5	5670	316	7.9	9.3	8.7

[a] Soils by World Reference Base classes ranked according to increasing soil weathering stage.
[b] Number of soils per group.
[c] Clay content data of highest clay yield.
[d] Soil organic carbon.
[e] Cation exchange capacity.
[f] Radiocaesium interception potential per unit clay of highest clay yield.
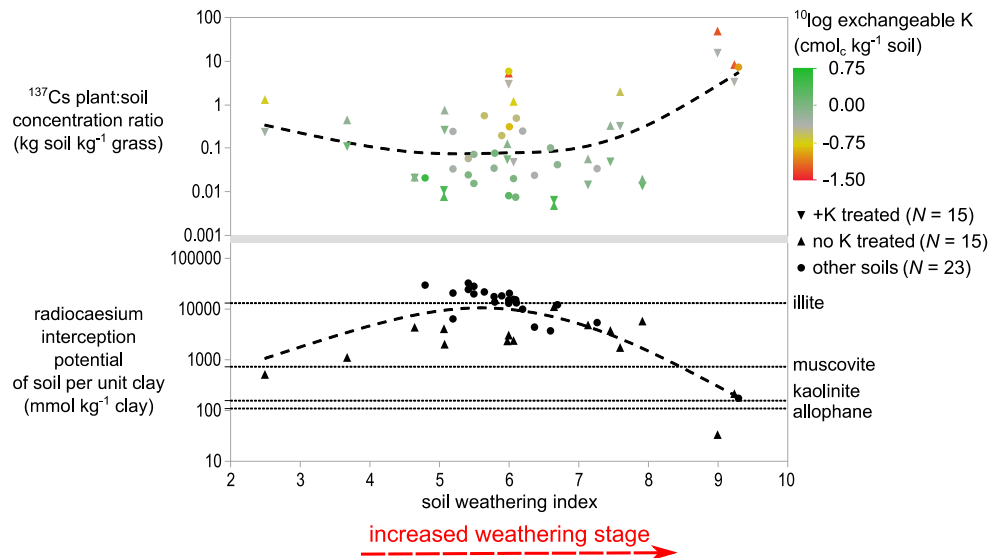
Fig. 1. Top: grass-soil ^{137}Cs concentrations ratios (log scale) in relation to calculated weathering index based on mineralogy. Data are combined from soils with (+K, $N = 15$) and without K (no K, $N = 15$) fertilizer treatment, in addition to those ($N = 23$) where K treatment was not assessed. Points on the graph are arithmetic mean CR values ($n = 3$) and are colored depending on exchangeable K content in soils (note log scale). Bottom: RIP of soil per unit clay (highest clay content) as soil weathering increases. The dotted lines are RIP of allophane (111 mmol kg^{-1}), illite (10,000–16,000 mmol kg^{-1} (De Koning, 2007; Wauters et al., 1996)), muscovite (740 mmol kg^{-1} (De Preter, 1990)) and kaolinite (6–310 mmol kg^{-1} (Nakao et al., 2008; Ogasawara et al., 2013)). The dashed lines are cubic spline regression curves ($\lambda = 3$, standardized) (Top: R$^2 = 0.36$, sum of squares error (SSE) = 32; Bottom: R$^2 = 0.69$, SSE = 7.9).

3.4. Single soil properties explained ^{137}Cs transfer

Soil properties such as organic C, clay content (highest clay content obtained by various methods) (Fig. 2(a)) or phyllosilicate content (Fig. A.7(a)) did not explain CR by single regression ($p > 0.05$).

However, clay content determined exclusively by the laser diffraction method explained 25 % of the CR, yet laser diffraction clay content underestimated the phyllosilicate content determined by XRD (Fig. A.7 (b)). The variability of CR was slightly influenced by soil pH (Fig. 2(b)) and, to a larger extent, by the NH$_4$ concentration in solution (R$^2 = 0.58$,
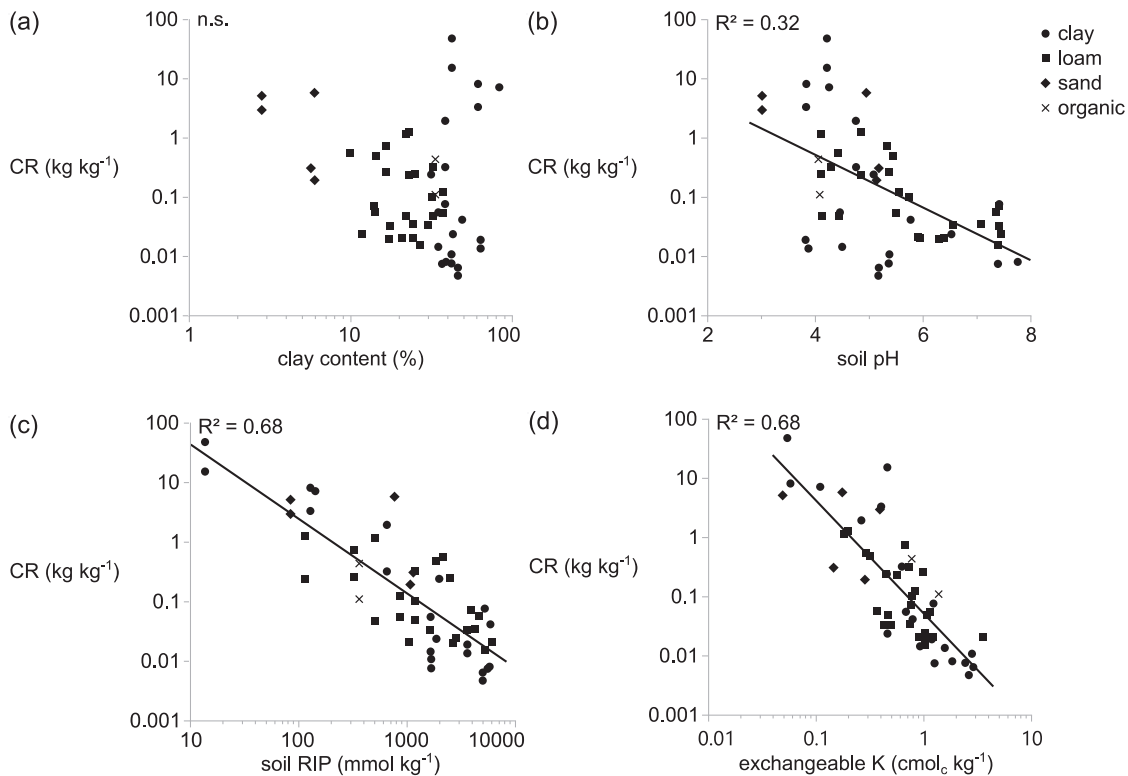

Fig. 2. Soil properties explaining the grass-soil ^{137}Cs concentration ratio CR ($N = 53$), which are (a) clay content (highest clay yield), (b) soil pH, (c) radiocaesium interception potential, and (d) exchangeable K content before plant growth. Points on the graphs are mean values ($n = 3$) which are marked according to the classification based on the clay, sand and organic matter contents (IAEA, 2009): clay (clay ≥35 %, circle), loam (18 % < clay <35 %, square), sand (sand ≥65 % and clay <18 %, diamond), and organic (organic matter ≥20 %, cross).

not shown). The RIP explained 68 % (Fig. 2(c)), and exchangeable K content before plant growth explained 68 % (Fig. 2(d)) of the CR. CR was better explained by the exchangeable K content after ($R^2 = 0.81$, RMSE = 0.41, $N = 24$) than before ($R^2 = 0.74$, RMSE = 0.48, $N = 24$) plant growth.

3.5. Soil solution ^{137}Cs and K explain ^{137}Cs uptake by plants

The ^{137}Cs transfer from soil to grass is largely controlled by ^{137}Cs concentration in soil solution and $^{137}Cs^+$:K^+ competition for plant uptake. Hence, the ^{137}Cs plant-solution concentration ratios (i.e. CF values) were well predicted by single linear regression with the K in solution ($R^2 = 0.69^{***}$, RMSE = 0.39) (Fig. 3).

3.6. ^{137}Cs soil-plant transfer predicted by existing models

The ^{137}Cs soil-to-plant transfer models of Absalom et al. (2001, 1999) and Tarsitano et al. (2011) were tested on the data in this study. The Absalom 2001 and Tarsitano 2011 models performed well (Table 2) for soils of various weathering stages (Fig. 4). The highest clay content values were used as model variables for consistency and because predictions were better (except for Absalom 1999, $R^2_{adj} = 0.28$, RMSE = 0.84, mean observed over predicted ratio (O/P) = 16,000). The largest underestimation of CR (mean $O/P = 5$–11) by the Absalom 2001 and Tarsitano 2011 models was for low RIP values (<1000 mmol kg^{-1}). This underestimation increased (mean $O/P = 7$–12) if laser diffraction clay contents were used. Although it predicted the CR satisfactorily, the Tarsitano 2011 model incorrectly predicted K concentration in soil solution (Fig. A.8(a)) and ^{137}Cs K_D in low RIP soils (Fig. A.8(b)). This suggest compensatory effects of both variables.

A regression model with the same soil property input variables performed better than the Absalom 2001 and Tarsitano 2011 models (Table 2). The prediction was further improved when RIP was included in the regression. The best regression model, using a stepwise mixed selection of variables ($p < 0.05$), was based on clay content, RIP, exchangeable K and NH$_4$ in soil solution.

4. Discussion

The contrasting parent materials and weathering stages of soils in this study affect mineralogy and, hence, RIP. The RIP/%clay are of the same order of magnitude for each soil class as previously reported in Vandebroek et al. (2011) (Fig. A.2), except the Kenyan Ferralsol with 2:1 phyllosilicates (Table A.2). Moreover, RIP/%clay values correspond well to the range of RIPs of pure clay minerals that dominate in soils at certain weathering stages (Fig. 1), such as illite in younger and kaolinite
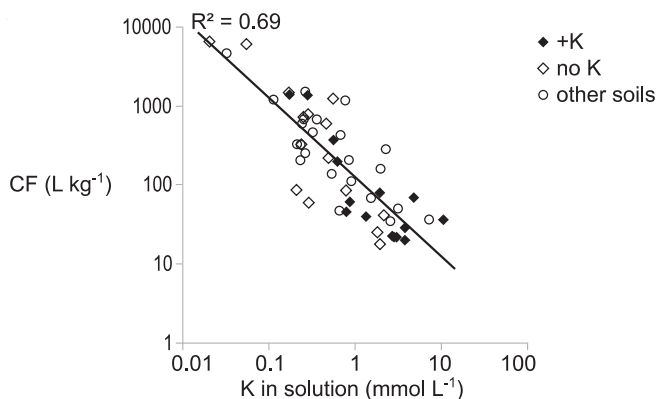

Fig. 3. The grass-soil solution ^{137}Cs concentration factor (CF) as a function of the solution K concentration ($N = 53$). Symbols indicate the K treatment. Points on the graphs are mean values ($n = 3$) and soil solutions are sampled before grass growth.

Table 2
Comparison of predicted ^{137}Cs grass-soil concentration ratios with the observed values ($N = 53$), all predictions were evaluated for log transformed CR values. Standard errors of estimates are given in brackets.

Model and soil variables in predictions	R^2_{adj}[g]	RMSE[h]	Mean O/P[i]
Absalom 1999 with %clay, K$_{exch}$	n.s.	0.96	98,000
Absalom 2001 with %clay, %SOC, pH, K$_{exch}$, NH$_{4,solution}$	0.77***	0.47	6.7
Tarsitano 2011 with %clay, %SOC, K$_{exch}$, NH$_{4,solution}$	**0.78***	**0.46**	**2.9**
$log_{10}CR = -0.88(0.37) + 0.091(0.245)log_{10}$%clay $+ 0.37(0.18)log_{10}$%SOC $- 1.4(0.2)log_{10}K_{exch} + 0.51(0.08)log_{10}NH_{4,solution} - 1.0(0.4)[log_{10}$%clay $- 1.4] \bullet [log_{10}K_{exch} + 0.22]$	0.83***	0.41	1.5
$log_{10}CR = 1.2(0.3) - 0.78(0.11)log_{10}RIP - 1.2(0.2)log_{10}K_{exch}$	0.84***	0.40	1.5
$log_{10}CR = 1.1(0.3) - 0.62(0.10)log_{10}RIP - 0.94(0.15)log_{10}K_{exch} + 0.29(0.07)log_{10}NH_{4,solution}$	0.88***	0.34	1.3
$log_{10}CR = 0.98(0.44) + 0.016(0.186)log_{10}$%clay $- 0.58(0.01)log_{10}RIP - 0.89(0.16)log_{10}K_{exch} + 0.34(0.07)log_{10}NH_{4,solution} - 0.49(0.22)[log_{10}$%clay $- 1.4] \bullet [log_{10}RIP - 3.0]$	0.89***	0.33	1.3

[g] Adjusted correlation coefficient and significance (*$p < 0.05$; **$p < 0.01$; ***$p < 0.001$; not significant (n.s.) for $p > 0.05$).
[h] Root mean square error.
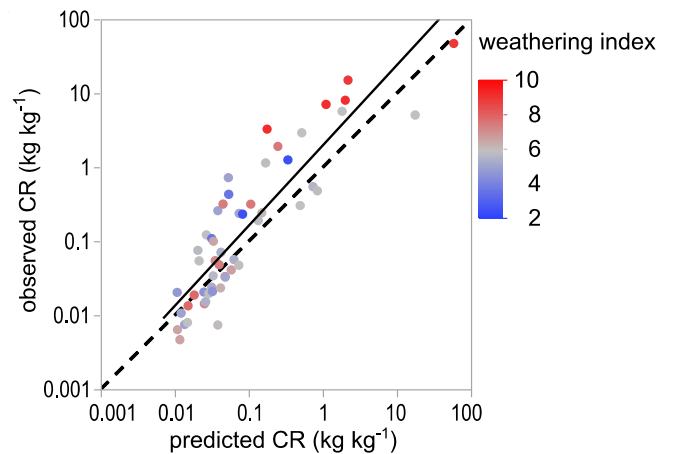[i] Mean observed over predicted ratio.

Fig. 4. Predictions of ^{137}Cs grass-soil concentration ratio with the Tarsitano 2011 model compared with observed CR values ($N = 53$). Points on the graph are mean CR values ($n = 3$). They are colored according to a calculated weathering index based on mineralogy, with the youngest (Andosols) equal to 2.5 (blue) and the oldest (Ferralsols) equal to 9.3 (red). The full line is the regression line, and the broken line is the 1:1 line.

in weathered soils.

The interpretation of data on a clay unit basis in relation to mineralogy critically depends on the clay isolation method that is, unfortunately, not standardized and rather operationally defined. Here, the clay content of a Ferralsol ranged from 9.7 % to 83 % (Table A.3) for different dispersion and measuring techniques. Moreover, using the same measurement technique, the clay content of that Ferralsol varied from 30 % to 44 % for different dispersion treatments (Table A.5). The standard WRB book of soil classification has no standardized protocol for the pretreatments aimed at complete dispersion of the primary particles (e.g. removal of iron as cementing material) and states that all such pretreatments are considered optional. These operational differences mainly affect the extremes of the weathering sequences, which are

young volcanic (Churchman and Tate, 1987) and weathered tropical soils (Bartoli et al., 1991).

The ^{137}Cs CR ranges over four orders of magnitude between 0.0047 and 47 kg kg^{-1} (Fig. 1). Overall, the CR values per soil class in this study are similar to those previously reported (IAEA, 2021; IAEA, 2020). However, the highest CR value obtained for one of the Ferralsols in this study is over 430–fold higher than the recently reported GM of CR for grass in tropical environments (0.11 kg kg^{-1}, $N = 16$) (IAEA, 2021). That CR is even higher than for Histosols (44 kg kg^{-1}, (Sanchez et al., 1999)), which were considered the soils with highest ^{137}Cs transfer risk after the Chornobyl accident. In contrast, there is also a Ferralsol for which the CR is similar to those of soils from temperate climates (0.013 kg kg^{-1}) in which 2:1 phyllosilicates (>10 %) have been observed (Table A.2; Table A.7). Within a WRB class, the variability in CR value was up to 3500–fold (Fig. A.4). It is questionable whether grouping CR values by soil texture or class (i.e., IAEA, 2021; IAEA, 2020; IAEA, 2009) provides a reliable estimate for ^{137}Cs bioavailability.

The CR values ordered by weathering stages reveal a decreasing and subsequently increasing trend in ^{137}Cs grass-soil transfer with the degree of weathering (Fig. 1). The trend of the RIP/%clay logically mirrors that trend, which is expected because ^{137}Cs adsorption selectivity changes due to soil weathering (Chorover et al., 1999). Young volcanic soils have a high CR (>1 kg kg^{-1}) due to limited weathering, so 2:1 phyllosilicates have few frayed edges, and consequently, selective adsorption of ^{137}Cs is limited. In contrast, more developed soils have low CRs (0.01 kg kg^{-1}) because weathering leads to the formation of frayed edges on 2:1 phyllosilicates. Weathered tropical soils have the highest CRs (>10 kg kg^{-1}) due to the dominance of 1:1 phyllosilicates with limited ^{137}Cs selective adsorption. The role of weathering is also clear within the soil sequences, with comparable parent material (Fig. A.5). In the sequence from Kenya, the proportion of 2:1 phyllosilicates increased with weathering (RIP/%clay increases, i.e. first stage of weathering). In the sequence from the Philippines, weathering increased the proportion of kaolinite (RIP/%clay decreases, i.e. second stage of weathering). In parallel, as mineral structures change during weathering, the K–buffering capacity of the soil changes, accompanied by a decrease of structural charge and release of K from mineral layers. Although no clear trend of change in K–buffer capacity with weathering was found for the soils in this study (Fig. A.6), changes in K–buffering capacity, along with RIP, likely contribute to the variation in CR values (Fig. 1).

Overall, the Tarsitano 2011 model can predict the ^{137}Cs grass transfer for soils of contrasting parent materials and weathering stages (Fig. 4; Table 2), despite the poor predictions of underlying processes, i. e. the K_D values of ^{137}Cs or the soil solution K concentrations (Fig. A.8). This is likely due to the model not being calibrated for these diverse soils. We expected that the ^{137}Cs transfer models made for soils from temperate regions would not work for soils from tropical regions. This suggest that the underlying processes have counteracting effects yielding good predictions of the CR. The Absalom 2001 and Tarsitano 2011 models disregard the effect of mineralogy on ^{137}Cs transfer to plants; they effectively assume a constant RIP value per unit clay, which is reasonable for temperate regions where 2:1 phyllosilicates dominate the clay fraction (Fig. 1; Table A.2). However, this assumption was unrealistic when predicting ^{137}Cs transfer from the volcanic and tropical soils, as the RIP/%clay in such soils was considerably lower than in the temperate soils (due to the absence of 2:1 phyllosilicates), resulting in underestimating ^{137}Cs transfer (Fig. 4). These models should be improved, given that linear models, which were fitted to the soils of this study, outperform them (Table 2).

Even with limited soil collection, this study highlights the potential for high soil-to-plant transfer of ^{137}Cs in tropical soils and the limited benefit of K fertilization as a countermeasure in such soils. Therefore, it is important to be able to predict ^{137}Cs transfer from these soils realistically to support risk assessment and remediation of contaminated sites on a global scale. Existing transfer models, such as the model of Tarsitano 2011, can predict short-term ^{137}Cs soil-to-grass transfer for soils

from contrasting parent materials and weathering stages, likely due to the predominant role of exchangeable K content of the soil. Hence, for risk assessment, it appears critical to have regional-specific information on exchangeable K, and this may be problematic to obtain for tropical weathered soils, as shown recently (Albinet et al., 2022). It is also clear that global mapping of ^{137}Cs risk needs more consensus on clay isolation methods, especially for tropical soils.

CRediT authorship contribution statement

Margot Vanheukelom: Conceptualization, Data curation, Formal analysis, Investigation, Methodology, Visualization, Writing – original draft, Writing – review & editing. **Lieve Sweeck:** Conceptualization, Funding acquisition, Investigation, Methodology, Project administration, Resources, Supervision, Validation, Writing – review & editing. **Talal Almahayni:** Conceptualization, Funding acquisition, Investigation, Methodology, Project administration, Resources, Supervision, Validation, Writing – review & editing. **Mara De Bruyn:** Data curation, Formal analysis, Methodology. **Pieter Steegmans:** Data curation, Formal analysis, Methodology. **Lore Fondu:** Data curation, Formal analysis, Methodology. **Axel Van Gompel:** Data curation, Formal analysis, Methodology. **May Van Hees:** Data curation, Formal analysis, Methodology. **Jean Wannijn:** Data curation, Formal analysis, Methodology. **Erik Smolders:** Conceptualization, Formal analysis, Funding acquisition, Investigation, Methodology, Project administration, Resources, Supervision, Visualization, Writing – original draft, Writing – review & editing.

Declaration of competing interest

The authors declare that they have no known competing financial interests or personal relationships that could have appeared to influence the work reported in this paper.

Data availability

The data underlying this study are available in the published article and its Supplementary information. The X-ray diffraction patterns are openly available: Vanheukelom, Margot (2024), "Vanheukelom2024_XRD-pattern", Mendeley Data, V3, doi: 10.17632/rvbgvrccrg.3.

Appendix A. Supplementary data

Supplementary data to this article can be found online at https://doi.

org/10.1016/j.scitotenv.2024.173583.

References

Absalom, J.P., Young, S.D., Crout, N.M.J., Nisbet, A.F., Woodman, R.F.M., Smolders, E., Gillett, A.G., 1999. Predicting soil to plant transfer of radiocesium using soil characteristics. Environ. Sci. Technol. 33, 1218–1223. https://doi.org/10.1021/es9808853.

Absalom, J.P., Young, S.D., Crout, N.M.J., Sanchez, A., Wright, S.M., Smolders, E., Nisbet, A.F., Gillett, A.G., 2001. Predicting the transfer of radiocaesium from organic soils to plants using soil characteristics. J. Environ. Radioact. 52, 31–43. https://doi.org/10.1016/S0265-931X(00) 00098-9.

Albinet, F., Peng, Y., Eguchi, T., Smolders, E., Dercon, G., 2022. Prediction of exchangeable potassium in soil through mid-infrared spectroscopy and deep learning: from prediction to explainability. Artif. Intell. Agric. 6, 230–241. https://doi.org/10.1016/j.aiia.2022.10.001.

Almahayni, T., Beresford, N.A., Crout, N.M.J., Sweeck, L., 2019. Fit-for-purpose modelling of radiocaesium soil-to-plant transfer for nuclear emergencies: a review. J. Environ. Radioact. 201, 58–66. https://doi.org/10.1016/j.jenvrad.2019.01.006.

Bartoli, F., Burtin, G., Herbillon, A.J., 1991. Disaggregation and clay dispersion of Oxisols: Na resin, a recommended methodology. Geoderma 49, 301–317. https://doi.org/10.1016/0016-7061(91)90082-5.

Beck, H.E., Zimmermann, N.E., McVicar, T.R., Vergopolan, N., Berg, A., Wood, E.F., 2018. Present and future köppen-Geiger climate classification maps at 1-km resolution. Sci. Data 5, 1–12. https://doi.org/10.1038/sdata.2018.214.

Chorover, J., DiChiaro, M.J., Chadwick, O.A., 1999. Structural charge and cesium retention in a Chronosequence of Tephritic soils. Soil Sci. Soc. Am. J. 63, 169–177. https://doi.org/10.2136/sssaj 1999.03615995006300010024x.

Churchman, G.J., Tate, K.R., 1987. Stability of aggregates of different size grades in allophanic soils from volcanic ash in New Zealand. J. Soil Sci. 38, 19–27. https://doi.org/10.1111/j.1365-2389.1987.tb02119.x.

Ciesielski, H., Sterckeman, T., 1997. Determination of cation exchange capacity and exchangeable cations in soils by means of cobalt hexamine trichloride. Effects of experimental conditions. Agronomie 17, 1–7. https://doi.org/10.1051/agro:19970101.

Cremers, A., Elsen, A., De Preter, P., Maes, A., 1988. Quantitative analysis of radiocaesium retention in soils. Nature 335, 247–249. https://doi.org/10.1038/335247a0.

De Bauw, P., Shimamura, E., Rakotoson, T., Andriamananjara, A., Verbeeck, M., Merckx, R., Smolders, E., 2021. Farm yard manure application mitigates aluminium toxicity and phosphorus deficiency for different upland rice genotypes. J. Agron. Crop Sci. 207, 148–162. https://doi.org/10.1111/jac.12436.

De Koning, A., 2007. Measuring the specific caesium sorption capacity of soils. sediments and clay minerals 22, 219–229. https://doi.org/10.1016/j.apgeochem.2006.07.013.

De Preter, P., 1990. Radiocesium retention in the aquatic, terrestrial and urban environment: a quantitative and unifying analysis. [doctoral dissertation, KU Leuven].

Doebelin, N., Kleeberg, R., 2015. Profex: a graphical user interface for the Rietveld refinement program BGMN. J. Appl. Crystallogr. 48, 1573–1580. https://doi.org/10.1107/S1600576715014685.

IAEA, 2009. Quantification of Radionuclide Transfer in Terrestrial and Freshwater Environments for Radiological Assessments, TECDOC Series. INTERNATIONAL ATOMIC ENERGY AGENCY, Vienna.

IAEA, 2020. Environmental Transfer of Radionuclides in Japan Following the Accident at the Fukushima Daiichi Nuclear Power Plant, TECDOC Series. INTERNATIONAL ATOMIC ENERGY AGENCY, Vienna.

IAEA, 2021. Soil–Plant Transfer of Radionuclides in Non-temperate Environments, TECDOC Series. INTERNATIONAL ATOMIC ENERGY AGENCY, Vienna.

ISO (International Organization for Standardization), 1998. Soil quality – Determination of particle size distribution in mineral soil material – Method by sieving and sedimentation. 1st ed. Geneva, Switzerland. Reference No.: ISO 11277:1998(E).

IUSS Working Group WRB, 2022. World Reference Base for soil resources. International soil classification system for naming soils and creating legends for soil maps. In: International Union of Soil Sciences (IUSS), Vienna, Austria, 4th edition.

Jackson, M.L., Sherman, G.D., 1953. Chemical weathering of minerals in soils. Adv. Agron. 5, 219–318. https://doi.org/10.1016/S0065-2113(08)60231-X.

Jackson, M.L., Tyler, S.A., Willis, A.L., Bourbeau, G.A., Pennington, R.P., 1948. Weathering sequence of clay-size minerals in soils and sediments. I: fundamental generalizations. J. Phys. Colloid Chem. 52, 1237–1260. https://doi.org/10.1021/j150463a015.

Moore, D.M., Reynolds, R.C.J., 1997. X-Ray diffraction and the Identification and analysis of clay minerals, 2nd ed. Oxford University Press.

Nakao, A., Thiry, Y., Funakawa, S., Kosaki, T., 2008. Characterization of the frayed edge site of micaceous minerals in soil clays influenced by different pedogenetic conditions in Japan and northern Thailand. Soil Sci. Plant Nutr. 54, 479–489. https://doi.org/10.1111/j.1747-0765.2008.00262.x.

Nakao, A., Uno, S., Yanai, J., Kubotera, H., Tanaka, R., Root, R.A., Kosaki, T., 2021. Distance-dependence from volcano for Asian dust inclusions in andosols: a key to control soil ability to retain radiocesium. Geoderma 385, 114889. https://doi.org/10.1016/j.geoderma.2020.114889.

Ogasawara, S., Nakao, A., Yanai, J., 2013. Radiocesium interception potential (RIP) of smectite and kaolin reference minerals containing illite (micaceous mineral) as impurity. Soil Sci. Plant Nutr. 59, 852–857. https://doi.org/10.1080/00380768.2013.862158.

Sanchez, A.L., Wright, S.M., Smolders, E., Naylor, C., Stevens, P.A., Kennedy, V.H., Dodd, B.A., Singleton, D.L., Barnett, C.L., 1999. High plant uptake of radiocesium from organic soils due to Cs mobility and low soil K content. Environ. Sci. Technol. 33, 2752–2757. https://doi.org/10.1021/es990058h.

Schofield, R.K., Wormald Taylor, A., Taylor, A.W., 1955. The measurement of soil pH. Soil Sci. Soc. Am. J. 19, 164–167. https://doi.org/10.2136/sssaj1955.03615995001900020013x.

Shoji, S., Takahashi, T., 2002. Environmental and agricultural significance of volcanic ash soils. Glob. Environ. Res. Ed. 6, 113–135.

Smolders, E., Van Den Brande, K., Merckx, R., 1997. Concentrations of 137Cs and K in soil solution plant availability of 137Cs in soils. Environ. Sci. Technol. 31, 3432–3438. https://doi.org/10.1021/es970113r.

Środoń, J., Drits, V.A., McCarty, D.K., Hsieh, J.C.C., Eberl, D.D., 2001. Quantitative x-ray diffraction analysis of clay-bearing rocks from random preparations. Clay Clay Miner. 49, 514–528.

Tarsitano, D., Young, S.D., Crout, N.M.J., 2011. Evaluating and reducing a model of radiocaesium soil-plant uptake. J. Environ. Radioact. 102, 262–269. https://doi.org/10.1016/j.jenvrad.2010.11.017.

USDA, 1954. Diagnosis and improvement of saline and alkali soils. Soil Science Society of America Journal. United States Departement of agriculture. Soil and Water Conservative Research Branch, Agricultural Research Service. https://doi.org/10.2136/sssaj1954.036159950018000 30032x.

Vandebroek, L., Van Hees, M., Delvaux, B., Spaargaren, O., Thiry, Y., 2011. Relevance of Radiocaesium Interception Potential (RIP) on a worldwide scale to assess soil vulnerability to 137Cs contamination. J. Environ. Radioact. 104, 87–93. https://doi.org/10.1016/j.jenvrad.2011.09.002.

Vanheukelom, M., Sweeck, L., Van Hees, M., Weyns, N., Van Orshoven, J., Smolders, E., 2022. Quantitative clay mineralogy predicts Radiocesium bioavailability to ryegrass grown on reconstituted soils. SSRN Electron. J. 873, 162372 https://doi.org/10.2139/ssrn.4309526.

Wauters, J., Vidal, M., Elsen, A., Cremers, A., 1996. Prediction of solid/liquid distribution coefficients of radiocaesium in soils and sediments. Part two: a new procedure for solid phase speciation of radiocaesium. Appl. Geochem. 11, 595–599. https://doi.org/10.1016/0883-2927(96)00028-5.

Zeelmaekers, E., 2011. Computerized Qualitative and Quantitative Clay Mineralogy: Introduction and Application to Known Geological Cases. K.U.Leuven. Faculteit Wetenschappen, Leuven. ISBN:978-90-8649-414-9.

Zhu, Y.-G.G., Smolders, E., 2000. Plant uptake of radiocaesium: a review of mechanisms, regulation and application. J. Exp. Bot. 51, 1635–1645. https://doi.org/10.1093/jexbot/51.351.1635.